

Stable absorbing boundary conditions for molecular dynamics in general domains

Xiaojie Wu ^{*} and Xiantao Li [†]

*Department of Mathematics,
Penn State University, University Park*

October 14, 2018

Abstract

A new type of absorbing boundary conditions for molecular dynamics simulations are presented. The exact boundary conditions for crystalline solids with harmonic approximation are expressed as a dynamic Dirichlet-to-Neumann (DtN) map. It connects the displacement of the atoms at the boundary to the traction on these atoms. The DtN map is valid for a domain with general geometry. To avoid evaluating the time convolution of the dynamic DtN map, we approximate the associated kernel function by rational functions in the Laplace domain. The parameters in the approximations are determined by interpolations. The explicit forms of the zeroth, first, and second order approximations will be presented. The stability of the molecular dynamics model, supplemented with these absorbing boundary conditions is established. Two numerical simulations are performed to demonstrate the effectiveness of the methods.

Keywords: Absorbing boundary conditions; Molecular dynamics; Wave propagations

1 Introduction

Absorbing boundary conditions (ABCs) are extremely important numerical tools [29, 6, 27] to efficiently simulate wave propagation phenomena in large or infinite domains. In these methods, the computational cost is greatly reduced by truncating the entire domain into a much smaller region of interest. The boundaries of the truncated region are specifically treated to retain the characteristics of the full system. Mathematically, an exact boundary condition (BC) can often be derived, which tends to be nonlocal. For instance, in the work

^{*}xxw139@psu.edu; Corresponding author

[†]xx112@psu.edu;

of Engquist and Majda [10], the exact BC is represented via pseudo-differential operators. They can be approximated by Padé approximations, which lead to local ABCs. Another popular approach is to introduce an artificial absorbing layer to facilitate the propagation to the exterior. The most well-known method of this type is the perfectly matched layer (PML) method, which is originally formulated by Berenger [4] for Maxwell’s equations.

In the context of molecular dynamics (MD), the role of the ABCs is again critical: typical MD simulations involve a huge number of atoms and the computation tends to be prohibitively expensive. Therefore, ABCs are much needed to minimize the computational cost. It is worthwhile to first point out that the ABCs for MD models are different from those for continuous PDEs, since the dispersion relations are quite different. There has been a lot of recent development of ABCs for MD models. There are mainly three approaches:

Exact ABCs. The exact ABC can be derived for planar boundaries using Fourier/Laplace transform, or the lattice Green’s functions [5, 37, 36, 32, 17]. The main computational challenge is due to the convolutional integral in time, which has to be evaluated at each step. To the best of our knowledge, the best solution is given by the rational approximation of the continuum Green’s function [28]. Nevertheless, these exact BCs are limited to planar boundaries, and the explicit forms break down at corners.

Approximate ABCs by minimizing the total phonon reflection. In this approach, the reflection coefficient [9, 8] is calculated at boundaries of the truncated region. An approximate ABC, typically with a small number of previous time steps involved, is sought by minimizing the total reflection, in the form of energy fluxes [23]. This idea is extended to the cases of finite temperature [24]. A similar idea is the matching boundary conditions, proposed by Tang and his co-workers in a series of works [39, 11, 31]. They assume that the time history kernel can be approximated by an artificial local boundary condition. The unknowns are determined by a matching procedure at some pre-selected wave numbers.

Discrete PML. The PML method was extended to MD models by To and Li [35, 18]. Another extension based on continuum PML was performed by Guddati and co-workers [14]. Their approach is based on Guddati’s previous work, perfectly matched discrete layers (PMDL) [13], which is a more accurate implementation of PML. Similar to continuous PML, discrete PML is adaptable to complex geometries, for example, one does not need to treat the corner issue explicitly. The main subtlety is how to determine the parameters in PML. For examples, if they are too small or too large, significant reflections will occur.

In this paper, we propose a systematic approach to formulate and approximate the ABCs for domains with general geometry. In particular, we adopt an impulse/response perspective. More specifically, the impulse corresponds to the displacement (or traction) of the atoms at the boundary, which will induce a mechanical field in the surround region. This influence will in turn exert a kick-back force on the atoms at the boundary. Therefore, the response, which would exhibit a history-dependence, corresponds to these forces (or displacement). This can be formulated more precisely using the dynamic Dirichlet-to-

Neumann (DtN) map. This idea has been pursued for the wave equation and Schrödinger equation in [16, 3, 15]. Our proposed method involves the following steps:

- (a) To convert the dynamics problem to a static one, we take the Laplace transform in time.
- (b) We reduce the computational domain by using an atomistic-based boundary element method (ABEM). This eliminates the degrees of freedom associated with the surrounding atoms.
- (c) The dynamic DtN map can be obtained by an inverse Laplace transform. Instead of implementing this exact ABC, we approximate the Laplace transform by rational functions.
- (d) The rational function approximation reduces the nonlocal ABCs to local ODEs, which can be easily implemented.

We emphasize that the use of the ABEM method in (a) allows us to treat domains with general geometry, including multi-connected domains. Meanwhile, since the full MD model is a Hamiltonian system, a naive approximation of the BCs can lead to a unstable model. Our observation is that the formulation via the DtN map in step (b) makes the stability analysis more amenable. The rational approximation in step (d) eliminates the need to perform an inverse Laplace transform numerically.

The layout of this paper is as follows. The exact ABC is presented in section 2. We discuss the evaluation of the DtN map, along with its approximation in section 3. The stability of the ABCs is established in section 4. The approximate ABC is extended to the nonlinear MD model under a partial-harmonic approximation in section 5. We present two numerical experiments to demonstrate the effectiveness of these methods in section 6.

2 The formulation of Absorbing Boundary Conditions

Consider a system with N atoms in a domain Ω . Atoms in the domain have positions denoted by \mathbf{X} and displacement \mathbf{u} . The entire domain Ω is divided into two regions Ω_I and Ω_{II} , $\Omega_I \cup \Omega_{II} = \Omega$, as illustrated by Fig. 1. Here Ω_I can be multi-connected regions, e.g., around multiple local lattice defects. Ω_I refers to the computational domain, where the MD model is actually being implemented, and Ω_{II} indicates the surrounding region that is to be removed. We denote \mathbf{u}_I as the displacement of atoms in Ω_I and \mathbf{u}_{II} as the displacement of atoms in Ω_{II} . $\dim(\mathbf{u}_I) = n_I$, and $\dim(\mathbf{u}_{II}) = n_{II}$. In realistic problems, Ω_{II} involves much more atoms than those in the region Ω_I , i.e., $n_{II} \gg n_I$.

The ABCs can be derived when the interactions with u_{II} are linear. The resulting BC would be effective, as long as such approximations are acceptable.

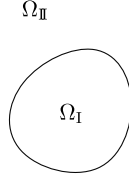


Figure 1: An illustration of the domain decomposition.

For the clarity of our formulation, we first assume that *all* the interactions are linear (In section 5, we will demonstrate that the formulation can be easily extended to the case where the interactions in Ω_I is nonlinear). This is the case where the formulation of the ABCs is most transparent. In this case, the potential energy of the system is quadratic, that is,

$$V = \frac{1}{2} \mathbf{u}^T D \mathbf{u}, \quad (1)$$

where $D_{ij} = \frac{\partial^2 V}{\partial \mathbf{u}_i \partial \mathbf{u}_j}$ corresponds to the Hessian matrix of the exact potential energy V in the MD model. Typically these models have short-range interactions, with the cut-off radius denoted by r_{cut} . This implies that $D = [D_{ij}]$ is a sparse matrix. In general, D is symmetric positive definite, due to the stability requirement.

Atoms in region Ω_I and Ω_{II} follow the equations of motion,

$$\begin{cases} \ddot{\mathbf{u}}_I = -D_{I,I} \mathbf{u}_I - D_{I,II} \mathbf{u}_{II}, \\ \ddot{\mathbf{u}}_{II} = -D_{II,I} \mathbf{u}_I - D_{II,II} \mathbf{u}_{II}. \end{cases} \quad (2)$$

Here, we set the mass to unity and defined $D_{I,I} = [D_{ij}]$, where $\mathbf{X}_i \in \Omega_I$, and $\mathbf{X}_j \in \Omega_I$. $D_{I,II}$, $D_{II,I}$, and $D_{II,II}$ are defined similarly. We have $D_{I,II} = D_{II,I}^T$. The dynamics (2) is stable, since the coefficient matrix

$$\begin{bmatrix} -D_{I,I} & -D_{I,II} \\ -D_{II,I} & -D_{II,II} \end{bmatrix}$$

is symmetric negative definite.

To build up the Dirichlet-to-Neumann (DtN) map, we take the Laplace transform of the second equation of (2) and get,

$$s^2 \mathbf{U}_{II} = -D_{II,I} \mathbf{U}_I - D_{II,II} \mathbf{U}_{II}, \quad s > 0, \quad (3)$$

where $\mathbf{U}_I(s) = \mathcal{L}\{\mathbf{u}_I(t)\}$, and $\mathbf{U}_{II}(s) = \mathcal{L}\{\mathbf{u}_{II}(t)\}$, which are the Laplace transforms of $\mathbf{u}_I(t)$ and $\mathbf{u}_{II}(t)$, respectively. Here, we assume that \mathbf{u}_I and \mathbf{u}_{II} are bounded functions, such that the Laplace transformations are well-defined. In the Laplace domain, we are able to formally solve the equations because $(s^2I + D_{II,II})$ is positive definite. The solution of Eq. (3) is the mapping from \mathbf{U}_{II} to \mathbf{U}_I , that is,

$$\mathbf{U}_{II} = -(s^2I + D_{II,II})^{-1}D_{II,I}\mathbf{U}_I. \quad (4)$$

In the time domain, Eq. (4) becomes,

$$\mathbf{u}_{II} = \int_0^t \beta(t-s)\mathbf{u}_I(s)ds, \quad (5)$$

where $\beta(s) = \mathcal{L}^{-1}\{B(t)\}$. Clearly, the matrix β has n_{II} rows, and it is too large to work with. Fortunately, the interactions have short range and this representation can be simplified to only involve atoms close to the boundary.

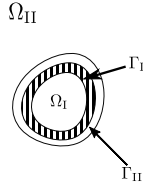


Figure 2: An illustration of the interface regions Γ_I and Γ_{II} .

The influence of \mathbf{u}_{II} on \mathbf{u}_I , $\mathbf{f}_{I,II} = -D_{I,II}\mathbf{u}_{II}$, corresponds to the Neumann boundary condition on Ω_I . Similarly, we define $\mathbf{f}_{II,I} = -D_{II,I}\mathbf{u}_I$ as the influence of \mathbf{u}_I on \mathbf{u}_{II} . Due to the short-range interactions and the translational invariance of the force constant matrices among the atoms, $D_{I,II}$ is a sparse matrix, that is, most entries in the matrices $D_{I,II}$ and $D_{II,I}$ are zeros. The following notations are motivated by the domain decomposition method, and they are useful to reveal the sparsity of the matrices and the nearsightedness of the interactions. We define the sets of boundary atoms as

$$\Gamma_I = \{i \in \Omega_I | D_{ij} \neq 0, \text{ for any } j \in \Omega_{II}\}, \text{ and } \Gamma_{II} = \{i \in \Omega_{II} | D_{ij} \neq 0, \text{ for any } j \in \Omega_I\}.$$

They are the collections of the atoms at the inner and outer boundaries, as indicated in Fig. (2). We now use $\mathbf{u}_{I,\Gamma}$ and $\mathbf{u}_{II,\Gamma}$ to represent the displacement of atoms in Γ_I and Γ_{II} , respectively. $\mathbf{u}_{I,\Gamma}$ has a dimension of m_I , and $\mathbf{u}_{II,\Gamma}$ has a dimension of m_{II} . We have $m_I, m_{II} \ll n_I$. With these notations, the short-range interactions can be revealed by writing the two matrices as

$$D_{I,II} = [D_{I,\Gamma} \quad \mathbf{0}], \text{ and } D_{II,I} = [D_{II,\Gamma} \quad \mathbf{0}]. \quad (6)$$

It is also natural to introduce the matrices E_I and E_{II} such that $\mathbf{u}_{I,\Gamma} = \mathbf{u}_I|_{\Gamma_I} = E_I \mathbf{u}_I$, and $\mathbf{u}_{II,\Gamma} = \mathbf{u}_{II}|_{\Gamma_{II}} = E_{II} \mathbf{u}_{II}$. Furthermore, we define $\mathbf{f}_{I,\Gamma} = -E_I D_{I,\Gamma} \mathbf{u}_{I,\Gamma}$, and $\mathbf{f}_{II,\Gamma} = -E_{II} D_{II,\Gamma} \mathbf{u}_{II,\Gamma}$ to denote the forces at the inner and outer boundaries.

equations	kernel functions	interpretations
$\mathbf{U}_{II,\Gamma} = B \mathbf{U}_{I,\Gamma}$	$B(s) = -E_{II}(s^2 I + D_{II,II})^{-1} D_{II,\Gamma}$	ABEM [22, 40] section: 3.2
$\mathbf{U}_{II,\Gamma} = \Theta \mathbf{F}_{II,\Gamma}$	$\Theta(s) = E_{II}(s^2 I + D_{II,II})^{-1} E_{II}^T$	Target kernel to approximate NtD map
$\mathbf{F}_{I,\Gamma} = T \mathbf{U}_{I,\Gamma}$,	$T(s) = D_{II,\Gamma}(s^2 I + D_{II,II})^{-1} D_{II,\Gamma}^T$	DtN map in Ω_{II} [30]
$\mathbf{F}_{I,\Gamma} = K s \mathbf{U}_{I,\Gamma} + \Theta(0) \mathbf{U}_{I,\Gamma}$	$K(s) = \frac{\Theta(s) - \Theta(0)}{s}$	GLE in Ω_{II} [7, 1]

Table 1: Kernel functions in the Laplace domain.

We now turn to the general forms of the boundary conditions. There are various ways to express the boundary conditions based on Eq. (4). Their forms in the Laplace domain are summarized in Table 1, along with references where these representations can be found. We will briefly go through the derivation of these formulas.

The first kernel function can be immediately obtained if we left-multiply both sides of Eq. (4) by E_{II} . This kernel function corresponds to a mapping between the displacement at the inner and outer boundaries.

To derive the second representation, one notices that the influence of \mathbf{u}_I on \mathbf{u}_{II} can be expressed as

$$\mathbf{f}_{II,I} = \begin{bmatrix} \mathbf{f}_{II,\Gamma} \\ \mathbf{0} \end{bmatrix}. \quad (7)$$

Further notice that the right hand side of Eq. (4) can be written as

$$(s^2 I + D_{II,II})^{-1} \mathbf{F}_{II,I} = [(s^2 I + D_{II,II})^{-1} E_{II}^T \quad *] \begin{bmatrix} \mathbf{F}_{II,\Gamma} \\ \mathbf{0} \end{bmatrix} = (s^2 I + D_{II,II})^{-1} E_{II}^T \mathbf{F}_{II,\Gamma}, \quad (8)$$

where $\mathbf{F}_{II,I}(s) = \mathcal{L}\{\mathbf{f}_{II,I}(t)\}$ is the Laplace transform of $\mathbf{f}_{II,I}(t)$, and $\mathbf{F}_{I,II}(s) = -D_{I,II} \mathbf{u}_{II}$ is the force from atoms in region Ω_I to atoms in region Ω_{II} .

To proceed, we left-multiply both sides of Eq. (4), and we get

$$\mathbf{U}_{II,\Gamma} = E_{II}(s^2 I + D_{II,II})^{-1} E_{II}^T \mathbf{F}_{II,\Gamma}. \quad (9)$$

This way, only the atoms outside the boundary are involved in Eq. (9). This DtN map connects the displacement and traction at the outer boundary. Numerically, the kernel function $\Theta(s)$ is amenable to numerical and analytical treatments, because it is symmetric positive definite for all s . (It is a principle submatrix of $(s^2 I + D_{II,II})$.) It is much more convenient to approximate a symmetric positive definite matrix-valued matrix by interpolations. The matrix $(s^2 I + D_{II,II})$ corresponds to a continuum screened Poisson operator or Klein-Gordon operator [2].

To arrive at the third expression, one can left-multiply $D_{\mathbb{I},\Gamma}$ to both sides of Eq. (4), which leads to,

$$\mathbf{F}_{\mathbb{I},\Gamma}(s) = D_{\mathbb{I},\Gamma}(s^2 I + D_{\mathbb{I},\mathbb{I}})^{-1} D_{\mathbb{I},\Gamma}^T \mathbf{U}_{\mathbb{I},\Gamma}(s). \quad (10)$$

In this case, the DtN operator is given by

$$T(s) = D_{\mathbb{I},\Gamma}(s^2 I + D_{\mathbb{I},\mathbb{I}})^{-1} D_{\mathbb{I},\Gamma}^T,$$

and it is a mapping between the displacement and traction at the inner boundary.

In the real-time domain, this DtN map is written as

$$\mathbf{f}_{\mathbb{I},\Gamma}(t) = \int_0^t \tau(t-s) \mathbf{u}_{\mathbb{I},\Gamma}(s) ds. \quad (11)$$

Here $\tau(t) = \mathcal{L}^{-1}\{T(s)\}$ is the inverse Laplace transform of $T(s)$. Fourier transformation versions of the expression (11) were discussed in [1, 7, 23].

Finally, the fourth expression in Table 1 can be obtained by writing,

$$\mathbf{F}_{\mathbb{I},\Gamma}(s) = \frac{T(s) - T(0)}{s} (s \mathbf{U}_{\mathbb{I},\Gamma}(s) - \mathbf{U}_{\mathbb{I},\Gamma}(0)) + T(0) \mathbf{U}_{\mathbb{I},\Gamma}(s), \quad (12)$$

and denote $K(s) = (T(s) - T(0))/s$. In the real-time domain, $\mathbf{f}_{\mathbb{I},\Gamma}$, accordingly, is expressed in terms of the *velocity* of the system. The alternative form of $\mathbf{f}_{\mathbb{I},\Gamma}$ is

$$\mathbf{f}_{\mathbb{I},\Gamma} = \int_0^t \kappa(t-s) \dot{\mathbf{u}}_{\mathbb{I},\Gamma}(s) ds - T(0) \mathbf{u}_{\mathbb{I},\Gamma}(t). \quad (13)$$

In the time domain, this derivation is equivalent to an integration by parts. In this form, the memory term can be viewed as a damping term, and it makes the stability analysis more straightforward [20].

In this paper, we choose the *second* expression of the DtN map, with kernel function $\Theta(s)$, to represent the boundary condition. The main reason is that the kernel function $\Theta(s)$ is symmetric positive definite for any value of $s > 0$, which may not hold in other three cases. Due to this property, some theoretical results can be easily established, and they are quite relevant to the stability of the boundary condition, which will be discussed in section 4. For convenience, we denote $\Theta_0 = \Theta(0)$, $\Theta_1 = \Theta(s_1)$, and $\Theta_2 = \Theta(s_2)$ for positive values of s_1 and s_2 .

Lemma 1. *For any $s_1 \neq s_2 > 0$, $(s_1^2(\Theta_1 - \Theta_0)^{-1} - s_2^2(\Theta_2 - \Theta_0)^{-1})/(s_1 - s_2)$ is symmetric negative definite.*

Proof. Let us consider

$$M = \frac{(s_1^2 I + D_{\mathbb{I},\mathbb{I}})^{-1} - (s_2^2 I + D_{\mathbb{I},\mathbb{I}})^{-1}}{s_1 - s_2}. \quad (14)$$

which is symmetric. Now, we show M is also negative definite. In fact, we can write M into a product of two matrices,

$$M = (s_1^2 I + D_{\mathbb{I}, \mathbb{I}})^{-1} \frac{s_2^2 - s_1^2}{s_1 - s_2} (s_2^2 + D_{\mathbb{I}, \mathbb{I}})^{-1}. \quad (15)$$

Both two matrices $(s_1^2 I + D_{\mathbb{I}, \mathbb{I}})^{-1}$ and $(s_2^2 I + D_{\mathbb{I}, \mathbb{I}})^{-1}$ are symmetric positive definite. Since M is symmetric, it follows immediately that M and $E_{\mathbb{I}} M E_{\mathbb{I}}^T$ are symmetric negative definite. Now, we consider

$$\begin{aligned} & \frac{s_1^2(\Theta_1 - \Theta_0)^{-1} - s_2^2(\Theta_2 - \Theta_0)^{-1}}{s_1 - s_2} \\ &= (\Theta_1 - \Theta_0)^{-1} \frac{s_1^2(\Theta_2 - \Theta_0) - s_2^2(\Theta_1 - \Theta_0)}{s_1 - s_2} (\Theta_2 - \Theta_0)^{-1} \quad (16) \\ &= (\Theta_1 - \Theta_0)^{-1} s_1^2 s_2^2 E_{\mathbb{I}} M E_{\mathbb{I}}^T D_{\mathbb{I}, \mathbb{I}}^{-1} (\Theta_2 - \Theta_0)^{-1}. \end{aligned}$$

Here $E_{\mathbb{I}} M E_{\mathbb{I}}^T D_{\mathbb{I}, \mathbb{I}}^{-1}$ is negative definite. In addition, $(\Theta_1 - \Theta_0)^{-1}$ and $(\Theta_2 - \Theta_0)^{-1}$ are symmetric negative definite. As a result, $(s_1^2(\Theta_1 - \Theta_0)^{-1} - s_2^2(\Theta_2 - \Theta_0)^{-1})/(s_1 - s_2)$ is symmetric negative definite. \square

Lemma 2. *If $0 < s_1 \neq s_2 < \sqrt{\lambda_{\min}(D_{\mathbb{I}, \mathbb{I}})}$, then $s_1(\Theta_2 - \Theta_0)^{-1} - s_2(\Theta_1 - \Theta_0)^{-1}/(s_1 - s_2)$ is positive definite.*

Proof. We will use the same technique as the proof of the last lemma. Let us consider

$$N = \frac{s_1(s_1^2 I + D_{\mathbb{I}, \mathbb{I}})^{-1} - s_2(s_2^2 I + D_{\mathbb{I}, \mathbb{I}})^{-1}}{s_1 - s_2}, \quad (17)$$

which is symmetric.

Left-multiplying N by $(s_1^2 I + D_{\mathbb{I}, \mathbb{I}})$ and right-multiplying N by $(s_2 I + D_{\mathbb{I}, \mathbb{I}})$, we get

$$\begin{aligned} N &= (s_1^2 I + D_{\mathbb{I}, \mathbb{I}})^{-1} \frac{s_1(s_2^2 I + D_{\mathbb{I}, \mathbb{I}}) - s_2(s_1^2 I + D_{\mathbb{I}, \mathbb{I}})}{s_1 - s_2} (s_2^2 + D_{\mathbb{I}, \mathbb{I}})^{-1} \\ &= (s_1^2 I + D_{\mathbb{I}, \mathbb{I}})^{-1} \frac{(s_1 - s_2)(-s_1 s_2 I + D_{\mathbb{I}, \mathbb{I}})}{s_1 - s_2} (s_2^2 + D_{\mathbb{I}, \mathbb{I}})^{-1}. \end{aligned} \quad (18)$$

Since $s_1 < \sqrt{\lambda_{\min}(D_{\mathbb{I}, \mathbb{I}})}$ and $s_2 < \sqrt{\lambda_{\min}(D_{\mathbb{I}, \mathbb{I}})}$, N is symmetric positive definite. Therefore,

$$\begin{aligned} & \frac{s_1(\Theta_2 - \Theta_0)^{-1} - s_2(\Theta_1 - \Theta_0)^{-1}}{s_1 - s_2} \\ &= (\Theta_1 - \Theta_0)^{-1} \frac{s_1(\Theta_2 - \Theta_0) - s_2(\Theta_1 - \Theta_0)}{s_1 - s_2} (\Theta_2 - \Theta_0)^{-1} \quad (19) \\ &= (\Theta_1 - \Theta_0)^{-1} s_1 s_2 E_{\mathbb{I}} N E_{\mathbb{I}}^T D_{\mathbb{I}, \mathbb{I}}^{-1} (\Theta_2 - \Theta_0)^{-1} \end{aligned}$$

is symmetric positive definite. \square

3 Approximations of the DtN map Θ

The direct evaluation of the DtN operator Θ is quite challenging. The difficulties of computation lie in two aspects: the inverse of a large matrix and infinitely many evaluations for frequency parameter s . In this section, the exact DtN map will be approximated by rational functions (section 3.1). We avoid the inverse of the large matrix by a domain reduction of the system. The domain reduction, in the form of the DtN map in the Laplace domain, will be discussed in section 3.2.

3.1 Approximation by Rational Functions

Instead of evaluating the time-dependent memory kernel, rational approximations can be made [10], which leads to dynamics without memory. In fact, the memory is eliminated via the introduction of a new variable. We consider the general form of the rational functions,

$$R_{n,n}(s) = (s^n I - s^{n-1}B_0 - \dots - B_{n-1})^{-1}(s^{n-1}A_0 + \dots + A_{n-1}), \quad (20)$$

where $A_i, B_i \in \mathbb{R}^{m_{\mathbb{I}} \times m_{\mathbb{I}}}$ for all $0 \leq i < n$. Notice that the dimension of the matrices A_i and B_i is small: $m_{\mathbb{I}} \ll n_{\mathbb{I}}$. The rational functions should satisfy $R_{n,n}(s) \approx \Theta(s)$. The form of the rational functions is inspired by the properties of the kernel function $\Theta(s)$: $\lim_{s \rightarrow \infty} \Theta(s) = 0$, and $\Theta'(0) = 0$. In our approximation, $\lim_{s \rightarrow \infty} R_{n,n}(s) = 0$ is automatically satisfied. For all following approximations, we always assume $R_{n,n}(0) = \Theta(0)$. This condition gives us

Assumption 1. $-B_{n-1}^{-1}A_{n-1} = \Theta_0$.

For higher order approximations, we may assume $R'_{n,n}(0) = \Theta'(0)$ to obtain the better approximation around zero. The first derivative condition leads to

Assumption 2. $-B_{n-1}^{-1}B_{n-2}B_{n-1}^{-1}A_{n-1} + B_{n-1}^{-1}A_{n-2} = 0$.

In this paper, we only show zeroth, first, and second order approximations. It is straightforward to extend the idea to high order cases. We define the approximation order as the degree of the polynomial in the denominator.

Zeroth order approximation. The zeroth order approximation is to use a constant matrix, which, according to Assumption 1, becomes $R_{0,0} = \Theta(0)$. One can also choose $s = s_0$ (s_0 is nonzero) as long as the corresponding dynamics is stable. In this paper, we make the intuitive choice $s = 0$. The approximate dynamics is reduced to

$$\ddot{\mathbf{u}}_{\mathbb{I}} = -D_{\mathbb{I},\mathbb{I}}\mathbf{u}_{\mathbb{I}} + E_{\mathbb{I}}^T D_{\mathbb{I},\Gamma}^T D_{\mathbb{I},\mathbb{I}}^{-1} D_{\mathbb{I},\Gamma} \mathbf{u}_{\mathbb{I},\Gamma}. \quad (21)$$

The stability of this approximation is shown in section 4. The dynamics can be further simplified by introducing $\bar{D}_{\mathbb{I},\mathbb{I}} = D_{\mathbb{I},\mathbb{I}} - E_{\mathbb{I}}^T D_{\mathbb{I},\Gamma}^T D_{\mathbb{I},\mathbb{I}}^{-1} D_{\mathbb{I},\Gamma} E_{\mathbb{I}}$. In practice, the interactions in $\Omega_{\mathbb{I}}$ are nonlinear, and $\bar{D}_{\mathbb{I},\mathbb{I}}$ never has to be computed. This will be discussed in the next section. Nonetheless, this Schur complement form

gives us the insight of the stability of the resulting dynamical system. The zeroth order approximation only involves the displacement of atoms in region Ω_I .

First order approximation. In this case, we consider the rational function,

$$R_{1,1}(s) = (sI - B_0)^{-1}A_0, \quad (22)$$

as the approximation. The coefficients A_0 and B_0 are determined by the interpolation at points $(s_0, \Theta(s_0))$ and $(0, \Theta(0))$, in accordance with Assumption 1. The corresponding approximate DtN map in real-time domain can be written as

$$\begin{aligned} \mathbf{u}_{\mathbb{I},\Gamma} &= \int_0^t e^{sB_0} A_0 \mathbf{f}_{\mathbb{I},\Gamma}(t-s) ds \\ &= -B_0^{-1} A_0 \mathbf{f}_{\mathbb{I},\Gamma}(t) + \int_0^t e^{sB_0} B_0^{-1} A_0 \dot{\mathbf{f}}_{\mathbb{I},\Gamma}(t-s) ds, \end{aligned} \quad (23)$$

which is similar to the alternative form (Eq. (13)) of the exact DtN map. We reformulate the approximate DtN map by integration by parts for the purpose of stability analysis in section 4. It is worth pointing out that, in this setting, $\mathbf{u}_{\mathbb{I},\Gamma}$ is expressed in terms of $\dot{\mathbf{f}}_{\mathbb{I},\Gamma}$. The term $-B_0^{-1} A_0 \mathbf{f}_{\mathbb{I},\Gamma}$, which according to Assumption 1, coincides with $\Theta(0) \mathbf{f}_{\mathbb{I},\Gamma}$ that will be moved to the first equation in Eq. (2). We denote $\mathbf{g} = \int_0^t e^{sB_0} B_0^{-1} A_0 \dot{\mathbf{f}}_{\mathbb{I},\Gamma}(t-s) ds$ and append the dynamics of \mathbf{g} to that of \mathbf{u}_I . The variable \mathbf{g} ($\mathbf{g} \in \mathbb{R}^{m_{\mathbb{I}} \times 1}$) is coupled with $\mathbf{v}_{I,\Gamma}$ only. With direct computation, one can verify that the approximate dynamics in this case is expressed as

$$\begin{cases} \ddot{\mathbf{u}}_I = -\bar{D}_{I,I} \mathbf{u}_I - D_{I,\Gamma} \mathbf{g}, \\ \dot{\mathbf{g}} = -B_0^{-1} A_0 D_{\mathbb{I},\Gamma} \mathbf{v}_{I,\Gamma} + B_0 \mathbf{g}, \end{cases} \quad (24)$$

where $\bar{D}_{I,I}$ has the same definition as the one in the zeroth order approximation.

Second order approximation. We express the second order rational approximation as

$$R_{2,2}(s) = (s^2 I - sB_0 - B_1)^{-1}(sA_0 + A_1). \quad (25)$$

The coefficients A_0 , A_1 , B_0 , and B_1 are determined by the interpolation among the values of $\Theta(s)$ and $\Theta'(s)$. In the second order approximation, we take both assumption 1 and assumption 2 into consideration. Two more values of $\Theta(s)$ will be used, at points $(s_1, \Theta(s_1))$ and $(s_2, \Theta(s_2))$, to determined those coefficients. In the real time domain, the corresponding approximate dynamics is

$$\ddot{\mathbf{u}}_{\mathbb{I},\Gamma} = B_0 \dot{\mathbf{u}}_{\mathbb{I},\Gamma} + B_1 \mathbf{u}_{\mathbb{I},\Gamma} + A_0 \dot{\mathbf{f}}_{\mathbb{I},\Gamma} + A_1 \mathbf{f}_{\mathbb{I},\Gamma}. \quad (26)$$

Equivalently, the above dynamics can be expressed as

$$\dot{\mathbf{w}} = B\mathbf{w} + A\mathbf{f}_{\mathbb{I},\Gamma}, \quad (27)$$

where $\mathbf{w} = \begin{bmatrix} \mathbf{u}_{\text{II},\Gamma} \\ \mathbf{z} \end{bmatrix}$, $B = \begin{bmatrix} B_0 & I \\ B_1 & \mathbf{0} \end{bmatrix}$, and $A = \begin{bmatrix} A_0 \\ A_1 \end{bmatrix}$. Employing the same technique in Eq. (23), we obtain

$$\mathbf{w} = -B^{-1}A\mathbf{f}_{\text{II},\Gamma}(t) + \int_0^t e^{sB}B^{-1}A\dot{\mathbf{f}}_{\text{II},\Gamma}(t-s)ds. \quad (28)$$

We denote $\mathbf{g} = \int_0^t e^{sB}B^{-1}AD_{\text{II},\Gamma}\dot{\mathbf{f}}_{\text{I},\Gamma}(t-s)ds$ and introduce the matrix E_1 (different from E_{I}) such that $\mathbf{f}_{\text{I},\text{II}} = E_1\mathbf{g}$. Then we can write an extended dynamics to represent the ABC:

$$\begin{cases} \ddot{\mathbf{u}}_{\text{I}} = -\bar{D}_{\text{I},\Gamma}\mathbf{u}_{\text{I}} - E_1D_{\text{I},\Gamma}\mathbf{g}, \\ \dot{\mathbf{g}} = -B^{-1}AD_{\text{II},\Gamma}\mathbf{v}_{\text{I},\Gamma} + B\mathbf{g}. \end{cases} \quad (29)$$

3.2 Evaluation of the DtN map

In practice, the sub-region Ω_{II} contains many atoms, but the region Ω_{I} contains much fewer atoms. As a result, the matrix $\Theta(s) \in \mathbb{R}^{m_{\text{II}} \times m_{\text{II}}}$ associated with the DtN map does not have a large dimension. However, it involves the inverse of $(s^2I + D_{\text{II}}) \in \mathbb{R}^{n_{\text{II}} \times n_{\text{II}}}$. The direction computation can be extremely expensive.

Fortunately, it is unnecessary to compute the entire inverse of $(s^2I + D_{\text{II},\text{II}})$. We only need to compute the Schur complement of the corresponding block of $(s^2I + D_{\text{II},\text{II}})$ for the atoms at the interface Γ . Thanks to the translation invariance of the force constant matrices, this calculation can be done very efficiently. We first consider the problem in the Laplace domain,

$$\tilde{D}_{\text{II},\text{II}}(s)\mathbf{U}_{\text{II}}(s) = \mathbf{F}_{\text{II},\text{I}}(s), \text{ for given } \mathbf{F}_{\text{II},\text{I}}(s) = -D_{\text{II},\text{I}}\mathbf{U}_{\text{I}}(s), \quad (30)$$

where $\tilde{D}_{ij} = D_{ij} + s^2\delta_{ij}I$. With the help of the lattice Green's function (A), the equation can be reduced to the degree of freedoms on the interface Γ by the atomistic-based boundary element method (ABEM) [22, 40]. In the original work, ABEM is implemented for static elasticity. In this paper, we extend the idea to dynamics problems where the force constant matrices are shifted by s^2I .

Since $\tilde{D} = [\tilde{D}_{ij}]$ is positive definite, the corresponding lattice Green's function is well-defined, which follows the relation $\sum_j \tilde{G}_{nj}\tilde{D}_{ji} = \delta_{ni}I$. The notation, $\tilde{\cdot}$, represents the variable in the Laplace domain. As a result, the displacement of atom n ($n \in \Omega_{\text{II}}$) can be trivially expressed as

$$\mathbf{U}_n = \sum_{i \in \Omega_{\text{II}}} \delta_{ni}\mathbf{U}_i = \sum_{i \in \Omega_{\text{II}}, j} \tilde{G}_{nj}\tilde{D}_{ji}\mathbf{U}_i. \quad (31)$$

The key step of the dimensional reduction is applying Abel's lemma (summation by parts) to Eq. (31). In this case, the Abel's lemma is expressed as

$$\sum_{i \in \Omega_{\text{II}}, j} \tilde{G}_{nj}\tilde{D}_{ji}\mathbf{U}_i = \sum_{i \in \Gamma_{\text{I}}, j \in \Gamma_{\text{II}}} \tilde{G}_{ni}D_{ji}\mathbf{U}_j - \sum_{i \in \Gamma_{\text{I}}, j \in \Gamma_{\text{II}}} \tilde{G}_{nj}D_{ji}\mathbf{U}_i + \sum_{j \in \Omega_{\text{II}}} \tilde{G}_{nj}\mathbf{B}_j, \quad (32)$$

where $\mathbf{B}_j = \sum_{i \in \Omega} D_{ji} \mathbf{U}_i$. In the above equation, the first two summations are over the interface Γ_I and Γ_{II} because of the locality of \tilde{D}_{ij} . When no external force is present, $\mathbf{B}_j = 0$. If we choose $n \in \Gamma_{II}$, Eq. (32) forms a linear system,

$$\mathbf{U}_{II,\Gamma} = \tilde{K} \mathbf{U}_{II,\Gamma} + \tilde{L} \mathbf{F}_{II,\Gamma}, \quad (33)$$

where

$$\begin{cases} \tilde{K}_{nj} = \sum_{i \in \Gamma_I} \tilde{G}_{ni} D_{ji} \\ \tilde{L}_{nj} = \tilde{G}_{nj} \end{cases} \quad (34)$$

The linear system is still closed. This linear system provides an alternative expression of the DtN map, given by

$$\mathbf{U}_{II,\Gamma}(s) = (I - \tilde{K}(s))^{-1} \tilde{L}(s) \mathbf{F}_{II,\Gamma}(s). \quad (35)$$

Notice that the matrices in the linear system have dimensions much smaller than n_{II} . Eq. (35), which provides the Schur complement of the corresponding block of the matrix $(s^2 I + D_{II,II})$, is equivalent to Eq. (9). In Eq. (35), we do not need to evaluate the inverse of a large matrix.

4 Stability of Absorbing Boundary Conditions (ABCs)

As a Hamiltonian system, the stability of the MD model after modifications due to the approximate BCs is a very delicate issue [33]. In this section, we will provide the principles of the approximations in section 3.1 to ensure stability. Since the coefficients of the rational approximation are determined by interpolation, our principles will focus on the selections of interpolation points.

Zeroth order approximation. The zeroth order approximation is automatically stable when we choose constant matrix $\Theta(0)$ as $R_{0,0}(s)$. In fact, $(D_{I,I} - E_I^T D_{II,\Gamma}^T D_{II,II}^{-1} D_{II,\Gamma})$ is the Schur complement of $D_{II,II}$ of symmetric positive definite matrix D . Therefore, we have the following stability condition of the dynamics (24).

Theorem 3 (Zeroth order approximation). *The zeroth-order approximate dynamics (Eq. (21)) is stable, provided that the interpolation point is $(0, \Theta(0))$.*

First order approximation. To establish the stability of Eq. (24), we introduce the following Lyapunov functional:

$$E(\mathbf{u}_I, \mathbf{v}_I, \mathbf{g}) = \frac{1}{2} \mathbf{v}_I^T \mathbf{v}_I + \frac{1}{2} \mathbf{u}_I^T \bar{D}_{I,I} \mathbf{u}_I - \frac{1}{2} \mathbf{g}^T A_0^{-1} B_0 \mathbf{g}. \quad (36)$$

Since $-A_0^{-1}B_0$ (Assumption 1) is symmetric positive definite, $E \geq 0$ for any \mathbf{v}_I , \mathbf{u}_I , and \mathbf{g} . The derivative of V ,

$$\begin{aligned} L_t E &= \mathbf{v}_I^T \dot{\mathbf{v}}_I + \mathbf{u}_I^T \bar{D}_{I,I} \dot{\mathbf{u}}_I - \mathbf{g}^T A_0^{-1} B_0 \dot{\mathbf{g}} \\ &= \mathbf{v}_I^T (-\bar{D}_{II} \mathbf{u}_I - D_{I,\Gamma} \mathbf{g}) + \mathbf{u}_I^T \bar{D}_{I,I} \dot{\mathbf{v}}_I - \mathbf{g}^T A_0^{-1} B_0 (-B_0^{-1} A_0 D_{II,\Gamma} \mathbf{v}_I + B_0 \mathbf{g}) \\ &= -\mathbf{g}^T A_0^{-1} B_0^2 \mathbf{g}. \end{aligned} \tag{37}$$

Hence, when $A_0^{-1}B_0^2$ is a positive semi-definite matrix, and $B_0^{-1}A_0$ (Assumption 1) is symmetric negative definite. According to standard ODE theory [33], the first order approximate dynamics (24) is stable.

Theorem 4 (First order approximation). *The approximate dynamics (24) is stable if the coefficients of the rational function (Eq. (22)) are determined by $R_{1,1}(0) = \Theta_0$ (Assumption 1) and $R_{1,1}(s_1) = \Theta_1$ with any $s_1 > 0$.*

Proof. The coefficients A_0 and B_0 are determined by solving the equations,

$$\begin{cases} -B_0^{-1}A_0 = \Theta_0, \\ (s_1 I - B_0)^{-1}A_0 = \Theta_1. \end{cases} \tag{38}$$

We eliminate the coefficient A_0 and have

$$(\Theta_1 - \Theta_0) B_0 = s_1 \Theta_1. \tag{39}$$

The matrix

$$\begin{aligned} \Theta_1 - \Theta_0 &= E_{II}(s_1^2 I + D_{II,II})^{-1} E_{II}^T - E_{II} D_{II,II}^{-1} E_{II}^T \\ &= -s_1^2 E_{II}(s_1^2 + D_{II,II})^{-1} D_{II,II}^{-1} E_{II}^T, \end{aligned} \tag{40}$$

is negative definite for any s_1 . As a result, $B_0 = s_1(\Theta_1 - \Theta_0)^{-1}\Theta_1$ is a negative definite matrix, and $A_0^{-1}B_0^2$ is a positive definite matrix. Therefore, the Lyapunov function defined by Eq. (36) is nonnegative, and its derivative $L_t E$ is semi negative definite. \square

Second order approximation. The stability of Eq. (29) will be analyzed in a similar approach as described in the first order case. The Lyapunov functional for the system (Eq. (29)) is defined by

$$E(\mathbf{u}_I, \mathbf{v}_I, \mathbf{g}) = \frac{1}{2} \mathbf{v}_I^T \mathbf{v}_I + \frac{1}{2} \mathbf{u}_I^T \bar{D}_{I,I} \mathbf{u}_I + \frac{1}{2} \mathbf{g}^T Q \mathbf{g}, \tag{41}$$

where

$$Q = \begin{bmatrix} -A_1^{-1} B_1 & \mathbf{0} \\ \mathbf{0} & A_1^{-1} \end{bmatrix}.$$

If $-A_1^{-1}B_1$ and A_1^{-1} are symmetric positive definite matrices, then Q is positive definite and the Lyapunov function is positive definite. The derivative of E is

$$\begin{aligned} L_t E &= \mathbf{v}_I^T \dot{\mathbf{v}}_I + \mathbf{u}_I^T \bar{D}_{I,I} \dot{\mathbf{u}}_I + \mathbf{g}^T Q \dot{\mathbf{g}} \\ &= -\mathbf{v}_I^T E_1 D_{I,\Gamma} \mathbf{g} - \mathbf{g}^T Q B^{-1} A D_{II,\Gamma} \mathbf{v}_I + \mathbf{g}^T Q B \mathbf{g} \\ &= \mathbf{g}^T Q B \mathbf{g}. \end{aligned} \tag{42}$$

Here, QB is explicitly expressed as

$$QB = \begin{bmatrix} -A_1^{-1}B_1B_0 & -A_1^{-1}B_1 \\ A_1^{-1}B_1 & \mathbf{0} \end{bmatrix}. \quad (43)$$

If QB is negative semi-definite, then $L_t E < 0$. QB is negative definite if and only if $-A_1^{-1}B_1B_0$ is negative definite. The stability conditions of dynamics (29) are that A_1^{-1} is symmetric positive definite, and $A_1^{-1}B_1B_0$ positive semi-definite.

Actually, these stability conditions are satisfied when we choose the interpolation points properly.

Theorem 5 (Second order approximation). *The approximate dynamics (29) is stable if the coefficients of the rational function Eq. (25) are determined by $R_{2,2}(0) = \Theta(0)$, $R'_{2,2}(0) = \Theta'(0)$, $R_{2,2}(s_0) = \Theta(s_0)$, and $R_{2,2}(s_1) = \Theta(s_1)$ with $0 < s_1 \neq s_2 < \sqrt{\lambda_{\min}(D_{II,II})}$.*

Proof. In fact, the coefficients A_0 , A_1 , B_0 , and B_1 are determined by solving a linear system,

$$-B_1^{-1}A_1 = \Theta_0, \quad (44a)$$

$$B_1^{-1}B_0B_1^{-1}A_1 - B_1^{-1}A_0 = 0, \quad (44b)$$

$$s_1B_0\Theta_1 + B_1\Theta_1 + s_1A_0 + A_1 = s_1^2\Theta_1, \quad (44c)$$

$$s_2B_0\Theta_2 + B_1\Theta_2 + s_2A_0 + A_1 = s_2^2\Theta_2, \quad (44d)$$

for the coefficients A_0 , A_1 , B_0 , and B_1 . Eq. (44b) (Assumption 2) is reduced to $A_0 = B_0B_1^{-1}A_1$. By solving the linear system for B_0 and B_1 , we have

$$B_0 = \frac{1}{s_1 - s_2} (s_1^2\Theta_1(\Theta_1 - \Theta_0)^{-1} - s_2^2\Theta_2(\Theta_2 - \Theta_0)^{-1}), \quad (45)$$

and

$$B_1 = \frac{s_1s_2}{s_2 - s_1} (s_1\Theta_1(\Theta_1 - \Theta_0)^{-1} - s_2\Theta_2(\Theta_2 - \Theta_0)^{-1}). \quad (46)$$

By Lemma 1, B_0 is positive definite. Since Θ_0 is symmetric positive definite, $A_1^{-1}B_1B_0$ is positive definite. By Lemma 2, B_1 is negative definite. Since $A_1 = -B_1\Theta_0$, we have that the coefficient,

$$A_1 = s_1s_2\Theta_0 - \frac{s_1s_2}{s_2 - s_1}\Theta_0 [s_1(\Theta_1 - \Theta_0)^{-1} - s_2(\Theta_2 - \Theta_0)^{-1}] \Theta_0 \quad (47)$$

is symmetric positive definite. Therefore, the dynamics (29) is stable. \square

5 Implementation of ABCs and partial-harmonic approximation of MD

For practical applications, the ABCs should be formulated so that the *nonlinear* interactions in Ω_I are retained, to properly model defect structure, formation,

and migration. This amounts to a *partial* harmonic approximation of the potential energy $V(\mathbf{u}_I, \mathbf{u}_{II})$. In this approximation, only the interactions involving the atoms in Ω_{II} are linearized. From the exact potential, these linear interactions should have coefficients given by

$$D_{I,II} = \frac{\partial^2 V}{\partial \mathbf{u}_I \partial \mathbf{u}_{II}}(\mathbf{0}, \mathbf{0}), \text{ and } D_{II,II} = \frac{\partial^2 V}{\partial \mathbf{u}_{II}^2}(\mathbf{0}, \mathbf{0}). \quad (48)$$

This is consistent with the notations in section 2. In particular, $D_{I,II}$ represents in the coupling between Ω_I and Ω_{II} .

The key observation is that when the region Ω_{II} is at mechanical equilibrium, we have $\mathbf{u}_{II} = C\mathbf{u}_I$ with $C = -D_{II,II}^{-1}D_{II,I}$, within the linear approximation. Notice that the equilibrium is relative to the displacement of the atoms in Ω_I . With this mechanical equilibrium as the references, we introduce the partial harmonic approximation by defining the following approximate potential energy:

$$\tilde{V}(\mathbf{u}_I, \mathbf{u}_{II}) = V(\mathbf{u}_I, C\mathbf{u}_I) + \frac{1}{2}(\mathbf{u}_{II} - C\mathbf{u}_I)^T D_{II,II}(\mathbf{u}_{II} - C\mathbf{u}_I). \quad (49)$$

The first part is the potential energy in Ω_I assuming a mechanical equilibrium in the surrounding area, while the second part is for region Ω_{II} .

We now show that this potential energy \tilde{V} is consistent with the exact model V in the following sense.

1. **\tilde{V} is a second order approximation.** More specifically, one can easily verify that,

$$\frac{\partial \tilde{V}}{\partial u_i}(\mathbf{0}, \mathbf{0}) = 0, \text{ for any } i \in \Omega, \quad (50)$$

and

$$\frac{\partial^2 \tilde{V}}{\partial u_i \partial u_j}(\mathbf{0}, \mathbf{0}) = D_{ij} = \frac{\partial^2 V}{\partial u_i \partial u_j}(\mathbf{0}, \mathbf{0}), \text{ for any } i, j \in \Omega. \quad (51)$$

This of course implies that $\tilde{V} = V$ if V is quadratic.

2. **The interactions in the interior of Ω_I is exactly preserved.** To see this property, we notice that most potential energy can be decomposed into site energies,

$$V = \sum_{i \in \Omega} V_i, \quad (52)$$

and V_i only depends on the atoms that are within the cut-off radius around the i -th atom. One can easily verify that, $V_i = \tilde{V}_i$ for all $i \in \Omega_I \setminus \Gamma_I$.

Applying the Hamilton's principle, we obtain the corresponding approximate dynamics,

$$\begin{cases} \ddot{\mathbf{u}}_I = -\nabla_{\mathbf{u}_I} V(\mathbf{u}_I, C\mathbf{u}_I) - C^T \nabla_{\mathbf{u}_{II}} V(\mathbf{u}_I, C\mathbf{u}_I) + C^T D_{II,II}(\mathbf{u}_{II} - C\mathbf{u}_I), \\ \ddot{\mathbf{u}}_{II} = -D_{II,II}\mathbf{u}_{II} - D_{II,I}\mathbf{u}_I. \end{cases} \quad (53)$$

Now, one can make the observation that the dynamics in Ω_{II} is identical to that in (2). Further more, the first equation is only coupled to \mathbf{u}_{II} linearly. These observations show that the DtN map can be formulated in the same way as in section 2. As an example, let us write out the molecular dynamics model in Ω_{I} , supplemented with the first order ABC,

$$\begin{cases} \ddot{\mathbf{u}}_{\text{I}} = -\nabla\Phi(\mathbf{u}_{\text{I}}) - D_{\text{I},\Gamma}\mathbf{g}, \\ \dot{\mathbf{g}} = -B_0^{-1}A_0D_{\text{II},\Gamma}\mathbf{v}_{\text{I},\Gamma} + B_0\mathbf{g}, \end{cases} \quad (54)$$

where $\Phi(\mathbf{u}_{\text{I}}) \stackrel{\text{def}}{=} V_{\text{I}}(\mathbf{u}_{\text{I}}, CE_{\text{I}}^T\mathbf{u}_{\text{I},\Gamma})$ is the effective potential energy in Ω_{I} .

It is also straightforward to establish the stability of the dynamics (54). We introduce this Lyapunov functional,

$$E = \Phi(\mathbf{u}_{\text{I}}) + \frac{1}{2}\mathbf{v}_{\text{I}}^T\mathbf{v}_{\text{I}} - \frac{1}{2}\mathbf{g}^T A_0^{-1}B_0\mathbf{g}. \quad (55)$$

Its derivative is simply given by,

$$L_t E = -\mathbf{g}^T A_0^{-1}B_0\mathbf{g}.$$

So the stability result still follows.

Since Ω_{II} involves many atoms, it is impracticable to evaluate the second term on the right hand side of the first equation in (53). But this term can be neglected. This can be justified by using an expansion,

$$\nabla_{\mathbf{u}_{\text{II}}}V(\mathbf{u}_{\text{I}}, C\mathbf{u}_{\text{I}}) \approx D_{\text{II},\text{II}}C\mathbf{u}_{\text{I}} + D_{\text{II},\text{I}}\mathbf{u}_{\text{I}} = \mathbf{0}.$$

The modeling error depends on the deformation of the system in Ω_{II} . In this paper, we will not provide the detailed proof. In fact,

$$\nabla_{\mathbf{u}_{\text{II}}}V(\mathbf{u}_{\text{I}}, C\mathbf{u}_{\text{I}}) = D_{\text{II},\text{II}}C\mathbf{u}_{\text{I}} + D_{\text{II},\text{I}}\mathbf{u}_{\text{I}} + H.O.T.$$

In light of the definition of the matrix C , the leading terms become zero.

6 Numerical simulations

In this section, we present the results from two molecular simulations with ABCs applied. The standard Verlet method is implemented for the time integration. The ABCs are simply discretized by the forward Euler method with the same time step size as the Verlet method. The time step of the simulations is set to be 76.2 femtoseconds ($10^{-15}s$).

System setup. We choose the nonlinear region $\Omega_{\text{I}} = [-50\text{\AA}, 50\text{\AA}] \times [-50\text{\AA}, 50\text{\AA}]$ and the surrounding region to be infinite $\Omega_{\text{II}} = \mathbb{R}^2 \setminus \Omega_{\text{I}}$. The region Ω_{I} is filled with 3,265 bcc iron atoms. The presence of the four corners does not impose any computational difficulty in our formulation. The periodic boundary condition is imposed in the z-direction to mimic a plane strain condition. Among the iron atoms, the interactions are modeled by the EAM potential [34]. As

preparations, the force constant matrices are approximated by standard finite difference formulas. Due to the locality of the computed force constant matrices, only 580 atoms in Ω_{II} and 520 atoms in Ω_{I} are involved in the evaluation of the DtN map $T(s)$. The calculation of the lattice Green’s function is discussed in the Appendix. For the initial configuration, the initial velocity is given by

$$v_x = 20 \sin(x/3)e^{-0.1r}, \text{ and } v_y = 20 \sin(y/3)e^{-0.1r}, \quad (56)$$

where $r = \sqrt{x^2 + y^2}$. The displacement of all atoms is zero initially.

Interpolation points. In all simulations, we apply zeroth, first, and second order approximate ABCs and monitor the wave reflections. For the zeroth order approximation, the only interpolation point is chosen as $s_0 = 0.1312$ PetaHz. For the first and second approximations, we need to solve a linear system for the coefficients of rational function. In practice, Assumption 1 can be extended to $-B_{n-1}^{-1}A_{n-1} = \Theta(s_0)$, where s_0 does not have to be zero. The proofs of stability still hold.

For the first order approximation, we choose $s_0 = 0.1312$ PetaHz and $s_1 = 0.2624$ PetaHz. For the second order approximation, $s_0 = 0.01312$ PetaHz, $s_1 = 0.1312$ PetaHz, and $s_2 = 0.3936$ PetaHz.

Performance. In implementing the proposed ABCs, only matrix-vector multiplications are involved in each time step, since the coefficients are determined a priori. Computation times were recorded (Table 2) when the three approximate ABCs are imposed on the same problem. We see that the higher order ABCs do not add up the computational cost significantly.

zeroth order	first order	second order
1979.108 s	2201.072 s	2783.020 s

Table 2: Computational time of the three approximate ABCs imposed on the same problem, same computer, for 200,000 time steps.

6.1 Waves in homogeneous systems

We observe within a short time period, the resulting velocity fields, under the three ABCs, are almost the identical. However, when the lattice waves arrive at the boundary, a complete reflection is observed under the zeroth order approximation. The reflection is reduced by the first order approximation. The second order approximation exhibited clear improvement: After several reflections, the lattice waves have been almost all absorbed.

6.2 Waves in a system with dislocations

In the second experiment, we implement the ABCs in a system with dislocations. The dislocations are created at $(-20\text{\AA}, 0)$ and $(20\text{\AA}, 0)$ by analytical solutions [25]. The Burgers vectors of the two dislocations are opposite in the same slip plane. In this case, the far-field displacement has fast decays. As preparations,

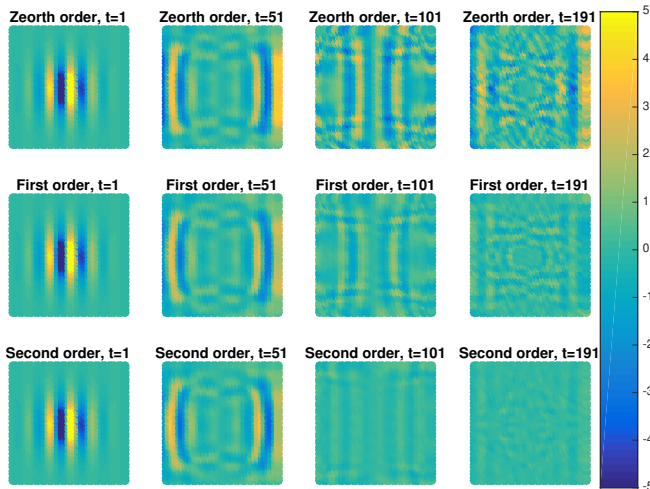


Figure 3: Wave propagations in the homogeneous system. The color indicates the velocity in the x direction.

the system is driven to an equilibrium state by minimizing the total energy. Then the same initial velocity is introduced. An interesting observation in this case is that high-frequency waves are generated by the interaction of the initial lattice waves and the dislocations. We observed that the second order approximation still performs the best. The reduction of the reflections is still significant.

7 Conclusion

In conclusion, we presented a new strategy to represent and approximate the ABCs systematically. It is a robust, efficient and easy-to-implement method to simulate phonons propagation in a large or infinite domain. Under this framework, further extensions can be pursued in various directions.

Finite temperature. In this paper, we only focused on the wave propagation at low temperature. Following the original idea of Adelman and Doll's work is based on generalized Langevin equation (GLE), and the great deal of recent development, the proposed ABCs can be extended naturally to the case of finite temperature. The extended approach will be able to exchange heat between truncated atomistic region and the bath.

Dynamical loading. Another important application of ABCs is to allow external elastic waves to come through the atomistic regions and interact with local defects, which is similar to [19]. Within the current framework, it means that a physical boundary needs to be included into the set Γ , where a dynamic

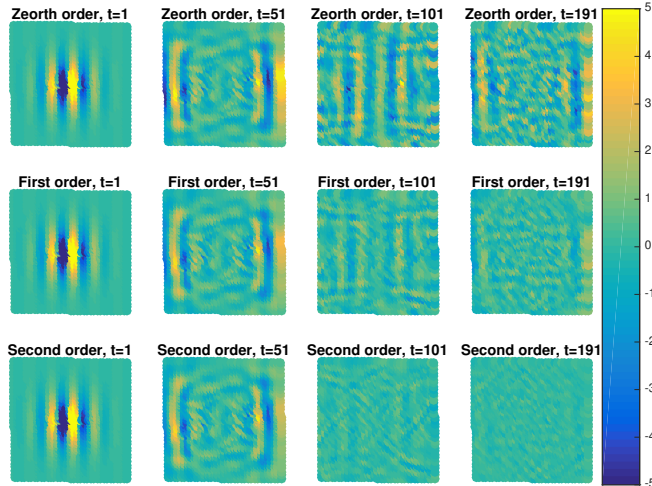


Figure 4: Wave propagations in the system with dislocations, the color indicates the value of velocity.

loading condition is applied. Another approach to include dynamic loading and simulation the propagation of elastic waves is to couple molecular dynamics models to a continuum elastic wave equation [21, 37]. In such a setting, the transparent boundary condition is still an important component.

A Lattice Green's function

The calculations of static lattice Green's functions were discussed in previous works [22, 40]. The integral expression of the lattice Green's function is numerically approximated by a quadrature formula over k -points. However, for the Green's function at long-distance, a direct calculation has to rely on a fine quadrature due to the high oscillations. Fortunately, it has been shown that the far-field lattice Green's function can be approximated by the continuum Green's function. The detailed proofs were provided in [26, 12]. In this paper, we focus on the calculation of the dynamics Green's function. An alternate form of the elastodynamic Green's function in Fourier space is given by C. -Y. Wang [38].

To explain the connection, let us consider the following 2D Fourier transform in terms of wave number $\boldsymbol{\xi}$:

$$\begin{aligned}
 F(\boldsymbol{\xi}) &= \mathcal{F}[f(\boldsymbol{x})] = \int_{\mathbb{R}^2} f(\boldsymbol{x}) e^{-i\boldsymbol{\xi}\cdot\boldsymbol{x}} d\boldsymbol{x}, \\
 f(\boldsymbol{x}) &= \mathcal{F}^{-1}[F(\boldsymbol{\xi})] = \frac{1}{4\pi^2} \int_{\mathbb{R}^2} F(\boldsymbol{\xi}) e^{i\boldsymbol{\xi}\cdot\boldsymbol{x}} d\boldsymbol{\xi}.
 \end{aligned} \tag{57}$$

We are seeking the fundamental solution to the *discrete* problem,

$$\ddot{\mathbf{u}}_i + \sum D_{ik} \mathbf{u}_k = \mathbf{f}_i. \quad (58)$$

The corresponding *continuum* problem is

$$(c_{ijkl} \partial_j \partial_l - \rho \delta_{jl} \partial_t^2) u_k = f_i, \quad (59)$$

where c_{ijkl} is the elastic constant. The elastic constant is connected to the force constant matrix, and the density ρ is related to the volume of unit cell. We may take the Laplace transforms of two problems,

$$(\Gamma_{ik}(\boldsymbol{\xi}) + \rho s^2 \delta_{ik}) U_k = F_i, \quad (60)$$

and

$$(D(\boldsymbol{\xi}) + s^2 I) \mathbf{U}_k = \mathbf{F}_i. \quad (61)$$

Here $\Gamma_{ik}(\boldsymbol{\xi}) = c_{ijkl} \xi_j \xi_l$. $D(\boldsymbol{\xi}) = \sum D_{\mathbf{R}} e^{-i\boldsymbol{\xi} \cdot \mathbf{R}}$ is the dynamic matrix for the discrete problem. Let us consider the Taylor expansion of $D(\boldsymbol{\xi})$,

$$\begin{aligned} D(\boldsymbol{\xi}) &\approx \sum_{\mathbf{R}} D_{\mathbf{R}} \left(1 - \frac{1}{2} (\boldsymbol{\xi} \cdot \mathbf{R})^2\right) \\ &= \left(-\frac{1}{2} \sum_{\mathbf{R}} D_{i-k} R_j R_l \xi_j \xi_l\right)_{ik}. \end{aligned} \quad (62)$$

The ξ^0 and ξ^1 terms disappear because of the inversion symmetry and the translation invariance. We see from direct comparison that the two problems are consistent with each other if

$$c_{ijkl} = -\frac{1}{2v_0} \sum_{\mathbf{R}} D_{i-k} R_j R_l, \quad (63)$$

where $v_0 = 1/\rho$ is the atomic unit volume.

Now, we show the connection between Green's functions of two above problems. The continuum Green's function is expressed as a Fourier integral,

$$G(\mathbf{x}, s) = \frac{1}{4\pi^2} \int_{\mathbb{R}^2} [\rho s^2 I + \Gamma(\boldsymbol{\xi})]^{-1} \cos(\boldsymbol{\xi} \cdot \mathbf{x}) d\boldsymbol{\xi}, \quad (64)$$

and the lattice Green's function is written as an integral over the first Brillouin zone,

$$G(\mathbf{R}_j, s) = \frac{1}{|B|} \int_B [s^2 I + D(\boldsymbol{\xi})]^{-1} \cos(\boldsymbol{\xi} \cdot \mathbf{R}_j) d\boldsymbol{\xi}. \quad (65)$$

Unlike static Green's functions, the matrices $s^2 I + D(\boldsymbol{\xi})$ and $\rho s^2 I + \Gamma(\boldsymbol{\xi})$ are positive definite. Hence, both Green's functions are uniquely defined. Formally, the lattice Green's function (65) converges to the continuum Green's function (64) when \mathbf{x} and \mathbf{R} are large enough, since only small $\boldsymbol{\xi}$ will contribute to the integral (65) in this regime.

The continuum dynamic Green's function can be further simplified for numerical evaluation. When we turn it to the polar coordinate, the continuum Green's function can be written as

$$G(\mathbf{x}, s) = \frac{1}{4\pi^2} \int_0^{2\pi} \int_0^{+\infty} [\rho s^2 I + r^2 \Gamma(\mathbf{n})]^{-1} \cos(r\mathbf{n} \cdot \mathbf{x}) r dr d\theta, \quad (66)$$

where $\mathbf{n} = (\cos \theta, \sin \theta)$. With the eigenvalue decomposition, the above expression of the continuum Green's function is written as

$$G(\mathbf{x}, s) = \frac{1}{4\pi^2} \int_0^{2\pi} \sum_i \int_0^{+\infty} \frac{\cos(r\mathbf{n} \cdot \mathbf{x}) r}{\rho s^2 + r^2 \rho c_i^2(\mathbf{n})} dr \mathbf{w}_i(\mathbf{n}) \otimes \mathbf{w}_i(\mathbf{n}) d\theta. \quad (67)$$

Here we wrote the i th eigenvalue of the matrix Γ as ρc_i^2 . The inner integral can be simplified to

$$\frac{1}{\rho c_i^2} \int_0^{+\infty} \frac{\cos(t|\mathbf{n} \cdot \mathbf{x}|s/c_i)}{1+t^2} dt = \frac{1}{\rho c_i^2} \left[\sinh(a_i) \text{Shi}(a_i) - \cosh(a_i) \text{Chi}(a_i) \right] \quad (68)$$

with $a = |\mathbf{n} \cdot \mathbf{x}|s/c_i$. In this formula, both $\sinh(a_i) \text{Shi}(a_i)$ and $\cosh(a_i) \text{Chi}(a_i)$ are increasing exponentially when $a_i > 0$. This expression may give us great round-off errors when we perform numerical simulations. But we can rearrange and simplify this expression as follows: By the properties of exponential integrals, $\text{Shi}(x) - \text{Chi}(x) = -\text{Ei}(-x)$, and $\text{Shi}(x) + \text{Chi}(x) = \text{Ei}(x)$ when s is positive, we have another form of the inner integral,

$$-\frac{1}{2\rho c_i^2} \left[e^{a_i} \text{Ei}(-a_i) + e^{-a_i} \text{Ei}(a_i) \right], \quad (69)$$

where $e^{a_i} \text{Ei}(-a_i)$ and $e^{-a_i} \text{Ei}(a_i)$ go to zero when $\|\mathbf{x}\|$ goes to infinity. This is more amenable to numerical evaluations.

It is interesting that this continuum Green's function is also connected to Wang's formula [38], where the dynamic Green's function in the time domain is given by

$$g(\mathbf{x}, t) = \frac{H(t)}{8\pi^2} \int_{|\mathbf{n}|=1} \sum_i \frac{P^i(\mathbf{n})}{\rho c_i} \left(\frac{1}{c_i t + |\mathbf{n} \cdot \mathbf{x}|} + \frac{1}{c_i t - |\mathbf{n} \cdot \mathbf{x}|} \right) d\mathbf{n}. \quad (70)$$

Here $P^i(\mathbf{n}) = \mathbf{w}_i(\mathbf{n}) \otimes \mathbf{w}_i(\mathbf{n})$. Even though our derivation differs from Wang's, both formulas are the integrals over unit circle. In fact, we take the Laplace transform of Eq. 70 when $|\mathbf{n} \cdot \mathbf{x}| \neq 0$,

$$G(\mathbf{x}, s) = -\frac{1}{4\pi^2} \int_0^{2\pi} \sum_i \frac{P^i}{\rho c_i^2} \left[\frac{e^{a_i} \text{Ei}(-a_i) + e^{-a_i} \text{Ei}(a_i)}{2} \right] d\theta. \quad (71)$$

Note that there is a singularity when $\mathbf{n} \cdot \mathbf{x} = 0$.

In the implementation, the singularity can be removed by adding another term inside the integral. More specifically,

$$G(\mathbf{x}, s) = -\frac{1}{4\pi^2} \int_0^{2\pi} \sum_i \frac{P^i}{\rho c_i^2} \left[\frac{e^{a_i} \text{Ei}(-a_i) + e^{-a_i} \text{Ei}(a_i)}{2} - \ln(|\mathbf{n} \cdot \mathbf{x}|) \right] d\theta - G(\mathbf{x}, 0), \quad (72)$$

where

$$\begin{aligned} G(\mathbf{x}, 0) &= -\frac{1}{4\pi^2} \int_0^{2\pi} \sum_i \frac{P^i}{\rho c_i^2} \ln(|\mathbf{n} \cdot \mathbf{x}|) d\theta \\ &= -\frac{1}{4\pi^2 \rho} \int_0^{2\pi} \Gamma^{-1}(\mathbf{n}) \ln(|\mathbf{n} \cdot \mathbf{x}|) d\theta, \end{aligned} \quad (73)$$

is the static Green's function for anisotropic solids, which according to the well known Stroh's formalism, can be expressed explicitly as,

$$G(\mathbf{x}, 0) = \frac{1}{\pi} \text{Im}(\ln(z_1) \mathbf{a}_1 \otimes \mathbf{a}_1 + \ln(z_2) \mathbf{a}_2 \otimes \mathbf{a}_2) + C, \quad (74)$$

where $z_1 = x_1 + \mu_1 x_2$ and $z_2 = x_1 + \mu_2 x_2$. μ_1 and μ_2 are the two roots to the sextic equation of elasticity, whose imaginary parts are positive. \mathbf{a}_1 and \mathbf{a}_2 are the two corresponding eigenvalues, and C is a constant. Using this subtraction, the integral in (72) can be easily evaluated.

References

References

- [1] S. A. Adelman and J. D. Doll. Generalized Langevin equation approach for atom/solid-surface scattering: Collinear atom/harmonic chain model. *The Journal of Chemical Physics*, 61(10):4242–4245, November 1974.
- [2] A. D. Alhaidari, H. Bahlouli, and A. Al-Hasan. Dirac and Klein–Gordon equations with equal scalar and vector potentials. *Physics Letters A*, 349(1):87–97, January 2006.
- [3] Bradley Alpert, Leslie Greengard, and Thomas Hagstrom. Nonreflecting Boundary Conditions for the Time-Dependent Wave Equation. *Journal of Computational Physics*, 180(1):270–296, July 2002.
- [4] Jean-Pierre Berenger. A perfectly matched layer for the absorption of electromagnetic waves. *Journal of Computational Physics*, 114(2):185–200, October 1994.
- [5] Wei Cai, Maurice de Koning, Vasily V. Bulatov, and Sidney Yip. Minimizing Boundary Reflections in Coupled-Domain Simulations. *Physical Review Letters*, 85(15):3213–3216, October 2000.

- [6] Robert Clayton and Björn Engquist. Absorbing boundary conditions for acoustic and elastic wave equations. *Bulletin of the Seismological Society of America*, 67(6):1529–1540, December 1977.
- [7] J. D. Doll and D. R. Dion. Generalized Langevin equation approach for atom/solid–surface scattering: Numerical techniques for Gaussian generalized Langevin dynamics. *The Journal of Chemical Physics*, 65(9):3762–3766, November 1976.
- [8] Weinan E and Zhongyi Huang. Matching Conditions in Atomistic-Continuum Modeling of Materials. *Physical Review Letters*, 87(13):135501, September 2001.
- [9] Weinan E and Zhongyi Huang. A Dynamic Atomistic–Continuum Method for the Simulation of Crystalline Materials. *Journal of Computational Physics*, 182(1):234–261, October 2002.
- [10] Bjorn Engquist and Andrew Majda. Absorbing Boundary Conditions for the Numerical Simulation of Waves. *Mathematics of Computation*, 31(139):629–651, 1977.
- [11] Ming Fang, Shaoqiang Tang, Zhihui Li, and Xianming Wang. Artificial boundary conditions for atomic simulations of face-centered-cubic lattice. *Computational Mechanics*, 50(5):645–655, November 2012.
- [12] M. Ghazisaeidi and D. R. Trinkle. Convergence rate for numerical computation of the lattice Green’s function. *Physical Review E*, 79(3):037701, March 2009.
- [13] Murthy N. Guddati and Keng-Wit Lim. Continued fraction absorbing boundary conditions for convex polygonal domains. *International Journal for Numerical Methods in Engineering*, 66(6):949–977, May 2006.
- [14] Murthy N. Guddati and Senganal Thirunavukkarasu. Phonon absorbing boundary conditions for molecular dynamics. *Journal of Computational Physics*, 228(21):8112–8134, November 2009.
- [15] Shidong Jiang and L Greengard. Fast evaluation of nonreflecting boundary conditions for the Schrödinger equation in one dimension. *Computers & Mathematics with Applications*, 47(6):955–966, March 2004.
- [16] Shidong Jiang and Leslie Greengard. Efficient representation of nonreflecting boundary conditions for the time-dependent Schrödinger equation in two dimensions. *Communications on Pure and Applied Mathematics*, 61(2):261–288, February 2008.
- [17] E. G. Karpov, G. J. Wagner, and Wing Kam Liu. A Green’s function approach to deriving non-reflecting boundary conditions in molecular dynamics simulations. *International Journal for Numerical Methods in Engineering*, 62(9):1250–1262, March 2005.

- [18] Shaofan Li, Xiaohu Liu, Ashutosh Agrawal, and Albert C. To. Perfectly matched multiscale simulations for discrete lattice systems: Extension to multiple dimensions. *Physical Review B*, 74(4):045418, July 2006.
- [19] X. Li. Variational boundary conditions for molecular dynamic in solids: treatment of the loading conditions. *J. Comp. Phys.*, 227:10078–10093, 2008.
- [20] X. Li. Stability of the boundary conditions for molecular dynamics. *J. Comp. Appl. Math.*, 231:493–505, 2009.
- [21] X. Li, J. Z. Yang, and W. E. A multiscale coupling for crystalline solids with application to dynamics of crack propagation. *J. Comp. Phys.*, 229:3970–3987, 2010.
- [22] Xiantao Li. An atomistic-based boundary element method for the reduction of molecular statics models. *Computer Methods in Applied Mechanics and Engineering*, 225(Supplement C):1–13, June 2012.
- [23] Xiantao Li and Weinan E. Variational boundary conditions for molecular dynamics simulations of solids at low temperature. *Communications in Computational Physics*, 1(1):135–175, 2006.
- [24] Xiantao Li and Weinan E. Variational boundary conditions for molecular dynamics simulations of crystalline solids at finite temperature: Treatment of the thermal bath. *Physical Review B*, 76(10):104107, September 2007.
- [25] Harold Liebowitz and Harold Liebowitz. *Fracture : An Advanced Treatise*. New York : Academic Press, 1968.
- [26] Per-Gunnar Martinsson and Gregory J. Rodin. Asymptotic Expansions of Lattice Green’s Functions. *Proceedings: Mathematical, Physical and Engineering Sciences*, 458(2027):2609–2622, 2002.
- [27] G. Mur. Absorbing Boundary Conditions for the Finite-Difference Approximation of the Time-Domain Electromagnetic-Field Equations. *IEEE Transactions on Electromagnetic Compatibility*, EMC-23(4):377–382, November 1981.
- [28] S. Namilaie, D. M. Nicholson, P. K. V. V. Nukala, C. Y. Gao, Y. N. Osetsky, and D. J. Keffer. Absorbing boundary conditions for molecular dynamics and multiscale modeling. *Physical Review B*, 76(14):144111, October 2007.
- [29] Daniel Neuhasuer and Michael Baer. The time-dependent Schrödinger equation: Application of absorbing boundary conditions. *The Journal of Chemical Physics*, 90(8):4351–4355, April 1989.
- [30] Assad A. Oberai, Manish Malhotra, and Peter M. Pinsky. On the implementation of the Dirichlet-to-Neumann radiation condition for iterative solution of the Helmholtz equation. *Applied Numerical Mathematics*, 27(4):443–464, August 1998.

- [31] Gang Pang, Songsong Ji, Yibo Yang, and Shaoqiang Tang. Eliminating corner effects in square lattice simulation. *Computational Mechanics*, pages 1–12, October 2017.
- [32] Harold S. Park, Eduard G. Karpov, and Wing Kam Liu. Non-reflecting boundary conditions for atomistic, continuum and coupled atomistic/continuum simulations. *International Journal for Numerical Methods in Engineering*, 64(2):237–259, September 2005.
- [33] Lawrence Perko. *Differential Equations and Dynamical Systems*. Springer Science & Business Media, November 2013. Google-Books-ID: VFnSB-wAAQBAJ.
- [34] Vijay Shastry and Diana Farkas. Molecular Statics Simulation Of Crack Propagation In A-Fe Using Eam Potentials. *MRS Online Proceedings Library Archive*, 409, January 1995.
- [35] Albert C. To and Shaofan Li. Perfectly matched multiscale simulations. *Physical Review B*, 72(3):035414, July 2005.
- [36] Gregory J. Wagner, Eduard G. Karpov, and Wing Kam Liu. Molecular dynamics boundary conditions for regular crystal lattices. *Computer Methods in Applied Mechanics and Engineering*, 193(17):1579–1601, May 2004.
- [37] Gregory J. Wagner and Wing Kam Liu. Coupling of atomistic and continuum simulations using a bridging scale decomposition. *Journal of Computational Physics*, 190(1):249–274, September 2003.
- [38] C.-Y. Wang and J. D. Achenbach. Elastodynamic fundamental solutions for anisotropic solids. *Geophysical Journal International*, 118(2):384–392, August 1994.
- [39] Xianming Wang and Shaoqiang Tang. Matching boundary conditions for diatomic chains. *Computational Mechanics*, 46(6):813–826, November 2010.
- [40] Xiaojie Wu and Xiantao Li. Simulations of Micron-scale Fracture using Atomistic-based Boundary Element Method. *Modelling and Simulation in Materials Science and Engineering*, 2017.